

# Control circuit for active power filter with an instantaneous reactive power control algorithm modification

**Abstract.** This paper describes a proposal for modifications to a shunt active power filter using a control circuit based on an instantaneous reactive power control algorithm. Such a control circuit has been realized using a fixed-point digital signal processor. When the value of load current changes rapidly, the APF transient response is too slow. This distortion causes an increase of harmonic content in the line current, which is dependent on a time constant. In the proposed circuit the transient performance of the APF is improved using non-causal predictive current compensation. Some illustrative, experimental results are also presented in the paper

**Streszczenie.** W artykule przedstawiono równoległy energetyczny filtr aktywny (APF) z algorytmem sterowania opartym na teorii mocy chwilowej. Układ sterowania zrealizowany został za pomocą stałoprzecinkowego procesora sygnałowego. Reakcja typowego równoległego filtra energetycznego na szybką zmianę prądu obciążenia jest zbyt wolna. Powoduje to zwiększenie zawartości harmonicznych w prądzie linii. W układzie sterowania zastosowano nieprzyczynowy algorytm sterowania. W pracy przedstawiono wyniki eksperymentalne opracowanej modyfikacji. (Układ sterowania energetycznym filtrem aktywnym z zastosowaniem zmodyfikowanego algorytmu opartego na teorii mocy chwilowej)

**Keywords:** shunt active power filter, digital signal processing (DSP), pulse width modulation (PWM).

**Słowa kluczowe:** równoległy energetyczny filtr aktywny, cyfrowe przetwarzanie sygnałów (CPS), modulacja szerokości impulsu (MSI).

## Introduction

Today most power network loads are nonlinear. Thus the shape of line voltage and current are not sinusoidal and they contain a lot of harmonics. To suppress power network harmonics, an active power harmonic compensator should be used; this compensator is also called an active power filter (APF). The APF can be connected in series or in parallel with the supply network. The series APF is applicable to the harmonic compensation of a large capacity diode rectifier with a DC link capacitor. The shunt APF (parallel APF) compensates the harmonics and asymmetries of the line currents caused by nonlinear loads.

The simplified diagram of a 75 kVA three-phase shunt active power filter test circuit is shown in Fig. 1. This APF has been built in our Institute laboratory and is used for testing APF control algorithms [3], [4]. The control circuit is based on a TMS320C50 fixed-point digital signal processor. The shunt APF (Fig. 1) control current dynamic is dependent on the inverter output time constant, itself resulting from the APF output inductance and resultant impedance of load and mains power line.

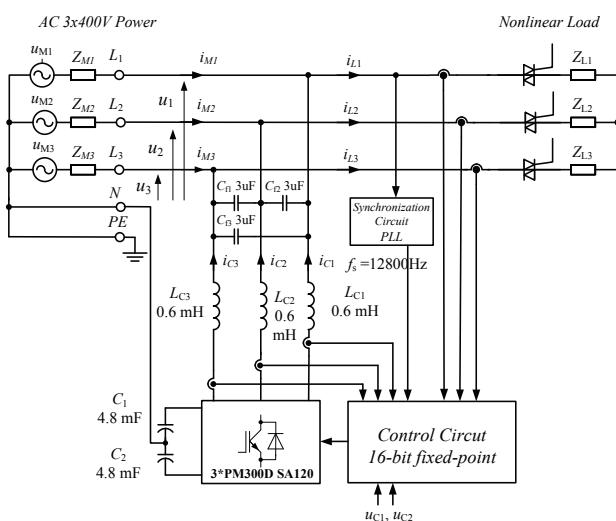


Fig. 1. Simplified diagram of compensation circuit with three-phase shunt active power filter (with unity gain)

When the value of load current changes rapidly, as in current  $i_L$  in Fig. 2, the APF transient response is too slow and the line current  $i_M$  suffers from dynamic distortion. This distortion causes an increase of harmonic content in the line current, which is dependent on a time constant. In the considered APF the total harmonic distortion (THD) ratio is increased by more than twelve percent.

The loads can be divided into two main categories: predictable loads and noise-like loads. Most loads belong to the first category. For this reason it is possible to predict current values in subsequent periods, after a few periods of observation [2], [5], [6], [7], [8].

## Instantaneous reactive power control algorithm

The control algorithm for the considered APF is based on the strategy resulting from the instantaneous reactive power theory initially developed by Akagi et al. [1], [9]. A simplified block diagram for the active power filter control algorithm is depicted in Fig. 3. The implementation of the control algorithm using a fixed-point 16-bit digital signal processor is described in detail by the author in [3], [4]. The digital signal processor is synchronized with the mains voltage  $u_1$  and the algorithm is performed  $N$  times per mains period. The sampling periods can be calculated with the formula

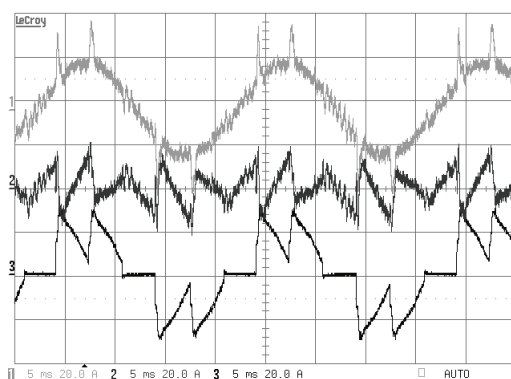


Fig. 2. Experimental waveforms of the classical three phase active power filter in steady-state with the resistive load: line current  $i_M$  (curve 1), compensating current  $i_C$  (curve 2), load current  $i_L$  (curve 3)

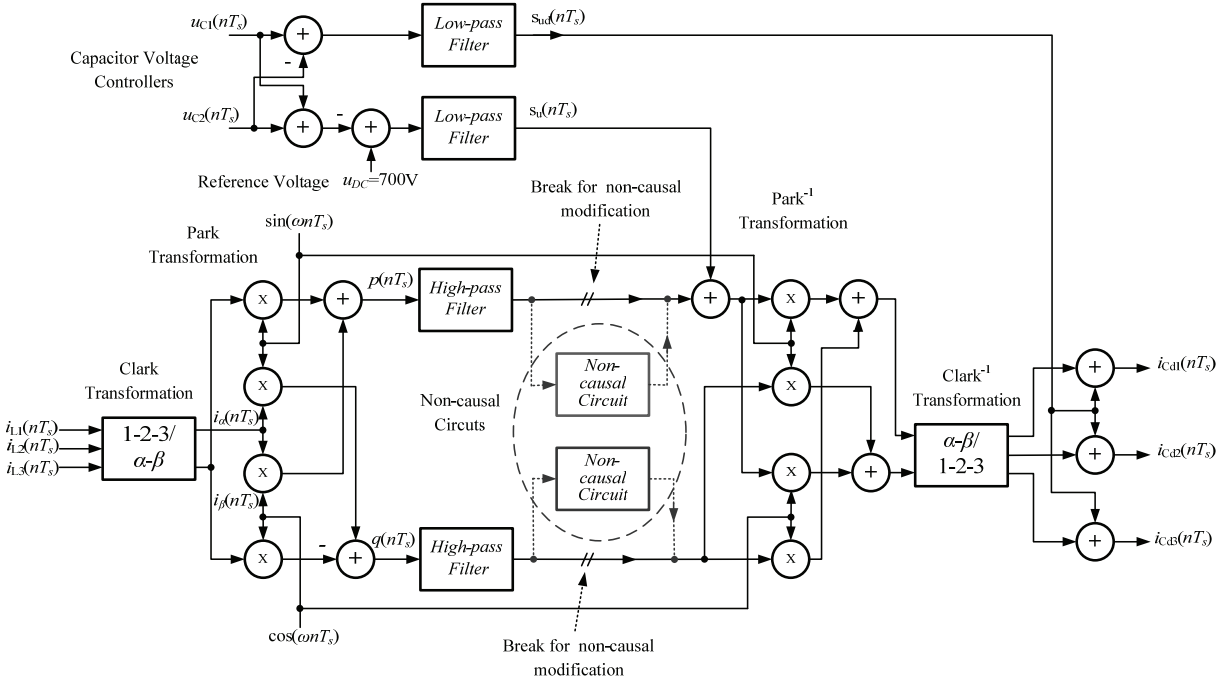


Fig. 3. Block diagram of instantaneous reactive power control algorithm

$$(1) \quad T_s = \frac{T_M}{N}$$

where:  $T_M$  – period of the line voltage,  $f_M = T_M^{-1}$  – frequency of the line voltage,  $N$  – number of samples per line period.

For the line voltage frequency of  $f_M=50$  Hz and the number of samples chosen being  $N=256$  the sampling period is equal to  $T_s = 78.125 \mu s$ , and the sampling rate is equal to  $f_s=12800$  samples/s.

A simplified block diagram of the control circuit and synchronization circuit is shown in Fig. 4. The sampling signal is produced by a phase lock loop circuit (PLL), which is connected to the line voltage  $u_1$  by a low-pass filter. This analogue filter suppresses distortion of the mains voltage by ensuring good synchronization and avoiding sampling signal jitter. Analogue input signals representing load currents:  $i_{L1}(t)$ ,  $i_{L2}(t)$ ,  $i_{L3}(t)$ , and DC bank (capacitors  $C_1$  and  $C_2$ ) voltages  $u_{C1}(t)$ ,  $u_{C2}(t)$  are sampled simultaneously by a 12-bit analog-to-digital converter with sampling ratio  $f_s$ . Therefore load currents are sampled at the same moment of time, and the time alignment jitter can be cancelled.

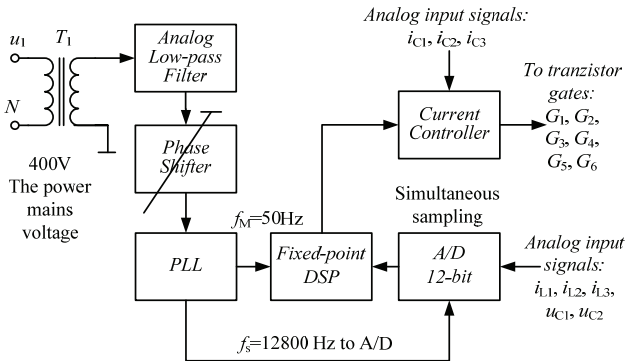


Fig. 4. Simplified block diagram of control circuit and synchronization circuit

### Modification

In the proposed solution, for predictable loads, it is possible to use a circuit with non-causal current compensation [5], [6], [7], [8], as shown in Fig. 3. The block diagram of the control circuit for one phase of the considered shunt APF is shown in Fig. 5 — for simplicity in this diagram the voltage controller is skipped. The desired digital compensation reference current signal  $i_{Cd}(nT_s)$  is sent to the non-causal circuit. Previous current compensation signal samples are stored in memory, and are sent to present output in advance. This compensation is dependent on the inverter output time constant. Because the time constant is mainly dependent on the output inverter inductor value it is possible to set a constant value for advance time  $T_A$ . In the considered APF the discrete advance time  $T_A$  is

$$(2) \quad T_A = N_{ah} T_s$$

where:  $N_{ah}$  – number of samples sent ahead.

The length of sample buffer can be calculated by the formula

$$(3) \quad L = N - N_{ah}$$

In the experimental circuit the advance time  $T_A$  is about several hundred microseconds [5], [6].

When the non-causal algorithm is switched on the compensation reference current signal sends samples ahead based on the last mains period. Finally, the output compensation reference current signal  $i_{Cdah}(t)$  is transformed to transistor controlling pulses by the current controller. In the considered circuit a hysteresis analogue current controller is employed. In such a solution the inverter switching speed depends largely on the load parameters. The hysteresis control algorithm is based on a nonlinear feedback loop with two-level hysteresis comparators. In the considered APF advanced analogue hysteresis a current controller with variable width hysteresis

is applied. This innovation gives additional improvements: maximum switching speed is limited, switching speed is dependent on the compensation reference current signals  $i_{Cd}$ ; the higher the signal level, the lower the switching speed.

Modification of the instantaneous reactive power control algorithm is shown in Fig. 3; to the classical control circuit are added two non-causal circuits - two simple delay lines, such as shown in Fig. 5.

Figures 6, 7 and 8 show the experimental waveforms in the same steady-state conditions, for the classical APF (Fig. 6) and for the modified APF circuit with non-causal predictive current compensation (Fig. 7 and 8). In these Figures are depicted the line currents  $i_{M1}$ ,  $i_{M2}$ ,  $i_{M3}$  and normalized spectra magnitude of one line current for

a different value of  $N_{ah} = \{2, 3\}$ . The best results are achieved for the number of samples sent ahead equaling three; for a higher number of samples the compensator is unstable. Using the new control algorithm with predictive harmonic compensation it is possible to decrease the harmonic contents in power line currents from around THD=14% to near THD=5% (for  $N_{ah} = 3$ ).

### Step response of APF

The first question for using the APF with a reactive power control algorithm with non-causal circuit is how it will work when the value of load current changes rapidly? For this reason step response of load currents for the considered shunt APF is investigated.

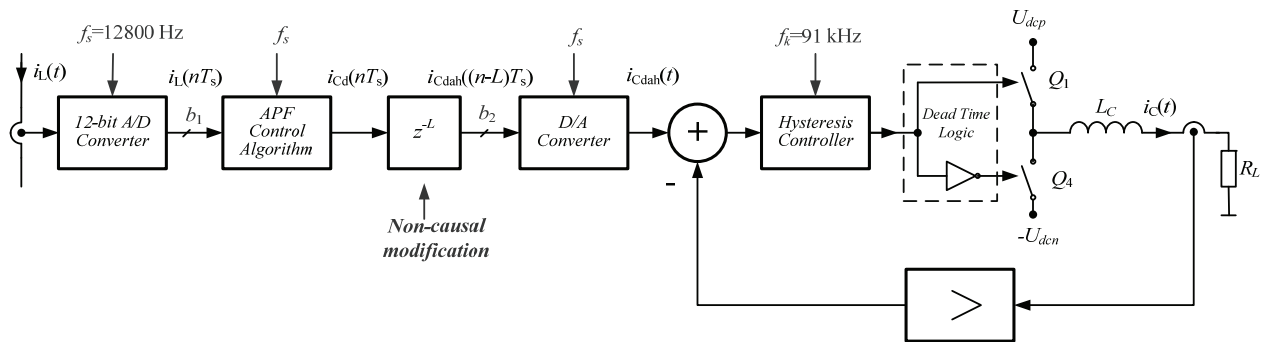


Fig. 5. Block diagram of control circuit for one phase of shunt APF

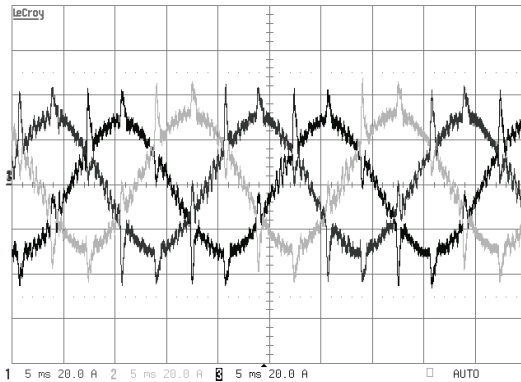


Fig. 6. Experimental waveforms of the classical three phase active power filter in steady-state with the resistive load, line currents:  $i_{M1}$ ,  $i_{M2}$ ,  $i_{M3}$ , normalized spectra magnitude of line current  $i_{M1}$

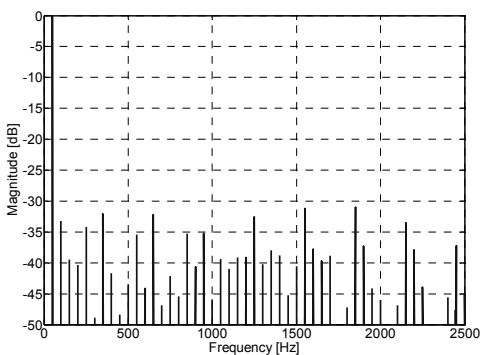
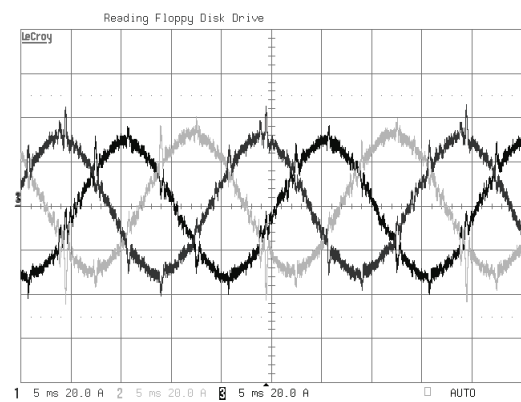
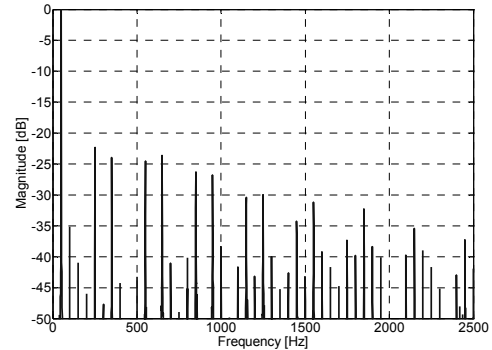


Fig. 7. Experimental waveforms of the modified three phase active power filter in steady-state with the resistive load for  $N_{ah} = 2$ , line currents:  $i_{M1}$ ,  $i_{M2}$ ,  $i_{M3}$ , normalized spectra magnitude of line current  $i_{M1}$

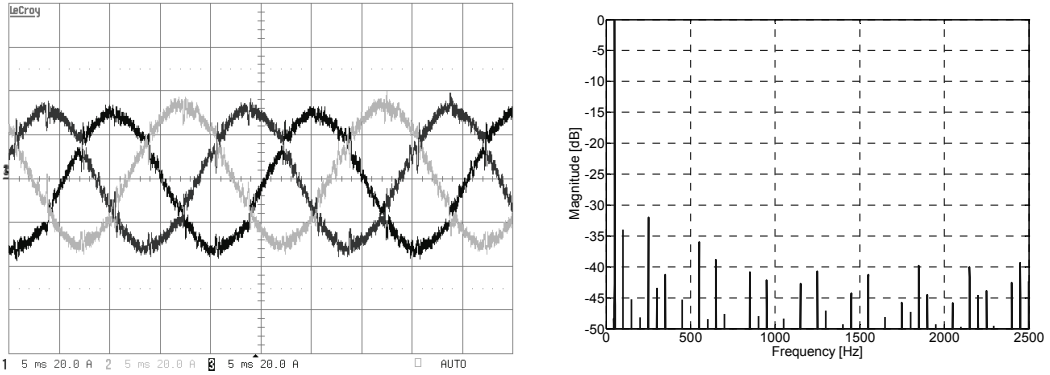


Fig. 8. Experimental waveforms of the modified three phase active power filter in steady-state with the resistive load for  $N_{ah} = 3$ , line currents:  $i_{M1}$ ,  $i_{M2}$ ,  $i_{M3}$ , normalized spectra magnitude of the line current  $i_{M1}$

Figure 9a shows the waveforms of a load current regulated by a power controller with resistive load without the APF compensation. The load current value is adjusted by a power controller regulated by thyristor phase control by changing trigger angle. The angle is controlled by square signal (curve 4, purple color) shown below in Fig. 9. The step response of the load currents for the considered shunt APF with classical control algorithm is shown in Fig. 9b, for the same load current values, as in Fig. 9a. The APF step response setting time is equal one period of line voltage. Figure 9c shows step response of the APF with modified control algorithm with non-causal circuits constantly switched on. In the first line voltage period, after the value of load currents are changed, the APF sends compensating current  $i_c$  adequate to previous load currents and the resultant currents are non-sinusoidal (Fig. 9c). Therefore

the non-causal circuit should be modified to circuit presented in Fig. 10 [10], [11], [5]. In this circuit current samples  $i_{in}(nT_s)$  are stored in DSP memory, in  $N$ -sample buffer and the next period of line current is compared with present samples, then if the absolute difference of present sample value and respective sample stored in memory is less than an assumed value the non-causal current compensation algorithm is switched on (switch  $S_1$  in position 1). To the output are sent non-causal samples  $i_{in}((n-L)T_s)$  from the buffer. If load current is changed the non-causal current predictive algorithm is switched off (switch  $S_1$  in position 2), and the algorithm waits for a steady-state and, when detected, it once again switches on (switch  $S_1$  in position 1). Waveforms with result of such modification is shown in Fig. 9d. After the rapid value of load current

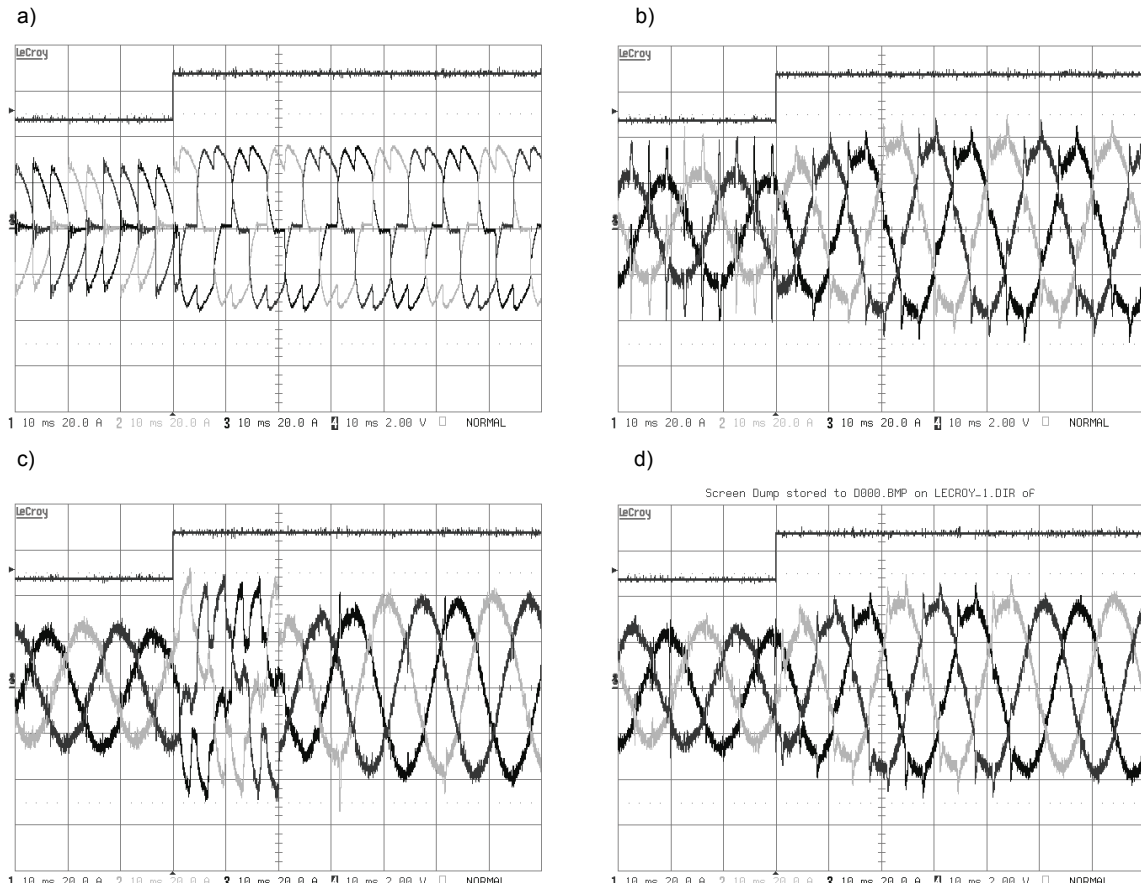


Fig. 9. Experimental waveforms of line currents:  $i_{M1}$ ,  $i_{M2}$ ,  $i_{M3}$  for step response of the load currents for the power controller with the resistive load: a) APF is switched off, b) APF with classical control algorithm, c) APF with non-causal algorithm constantly switched on,  $N_{ah} = 3$ , d) APF with adaptive non-causal algorithm,  $N_{ah} = 3$

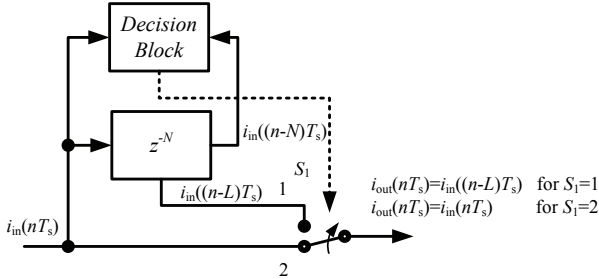


Fig. 10. Block diagram of non-causal circuit

changes the non-causal circuits are switched off. In the considered case (Fig. 9d), it is again switched on after two and half line voltage periods.

In considered shunt APF capacitance values of DC capacitors are very large, therefore DC voltage ripples are very small and they are not presented in this paper.

### Conclusion

Using non-causal predictive current compensation it is possible to decrease harmonics contents for predictable loads. This modification for an instantaneous reactive power control algorithm is very simple and additional computational workload is very small. Therefore it is easy to implement in an existing control circuit based on: digital signal processor, microcontroller or programmable digital circuit (FPGA, CLD, etc.). This simple modification can be easily implemented in existing APF digital control circuits, improving the quality of harmonics compensation.

### REFERENCES

- [1] H. Akagi, Y. Kanazawa, and A. Nabae, Instantaneous reactive power compensators comprising switching devices without energy storage components, *IEEE Transaction on Industry Application*, Vol. IA-20, May/June 1984, pp. 625–630.
- [2] S. Mariethoz, A. Rufer, Open Loop and Closed Loop Spectral Frequency Active Filtering, *IEEE Transactions on Power Electronics*, Vol.17, No 4, July 2002.
- [3] R. Strzelecki, Z. Fedyczak, K. Sozański, J. Rusiński, Energetyczne filtry aktywne EFA1, opis techniczny, *Instytut Elektrotechniki Przemysłowej*, Politechnika Zielonogórska, Zielona Góra, 2000. (in polish)
- [4] K. Sozański, R. Strzelecki, A. Kempski, Digital Control Circuit for Active Power Filter with Modified Instantaneous Reactive Power Control, *Algorithm, 33rd Annual IEEE Power Electronics Specialists Conference - PESC '02*, Cairns, Australia, 2002.
- [5] K. Sozański, Control algorithms with non-causal current predictor for active power filters, In: *Sterowanie w Energoelektronice i Napędzie Elektrycznym - SENE 2003 : VI krajowa konferencja naukowa*. Łódź, Polska, 2003, pp. 551–556.
- [6] K. Sozański, Non-causal current predictor for active power filter, *Nineteenth Annual IEEE Applied Power Electronics Conference and Exhibition, APEC 2004*, Anaheim, USA, 2004.
- [7] K. Sozański, The Shunt Active Power Filter with Better Dynamic Performance, *Power Tech 2007 Conference*, Lausanne, Switzerland, 2007.
- [8] K. Sozański, Shunt active power filter with improved dynamic performance, *13th International Power Electronics and Motion Control Conference - EPE-PEMC 2008*, Poznań, Polska, (2008), pp. 2018-2022.
- [9] H. Akagi, E. H. Watanabe, and M. Arede, Instantaneous Power theory and Applications to Power Conditioning, *Wiley-Interscience a John Wiley & Sons, Inc.*, Publication, 2007.
- [10] K. Sozański, *Improved Shunt Active Power Filters*, *Przegląd Elektrotechniczny (Electrical Review)*, 2008, nr 11, pp. 290-294.
- [11] K. Sozański, Realization of a shunt active power filter with improved dynamic performance, *Przegląd Elektrotechniczny (Electrical Review)*, 2009, nr 7, pp. 163-167.

**Author:** dr inż. Krzysztof Sozański, University of Zielona Góra, Institute of Electrical Engineering, ul. Podgórska 50, 65-246 Zielona Góra, E-mail: [K.Sozanski@iee.uz.zgora.pl](mailto:K.Sozanski@iee.uz.zgora.pl); [www.uz.zgora.pl/~ksozansk](http://www.uz.zgora.pl/~ksozansk)